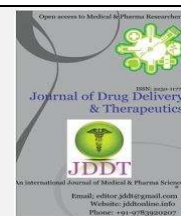


Available online on 15.06.2019 at <http://jddtonline.info>

# Journal of Drug Delivery and Therapeutics

Open Access to Pharmaceutical and Medical Research

© 2011-18, publisher and licensee JDDT, This is an Open Access article which permits unrestricted non-commercial use, provided the original work is properly cited

Open  Access

Research Article

## Fabrication and optimization of buccal film comprising rizatriptan benzoate loaded solid lipid nanoparticles for improved ex vivo permeation

Pramod Salve\*, Nikhil Bali

Nanotechnology Laboratory, University Department of Pharmaceutical Sciences, Rashtrasant Tukadoji Maharaj Nagpur University, Nagpur-440033, Maharashtra, India

### ABSTRACT

The objective of the present study was to fabricate and optimize mucoadhesive buccal film encloses rizatriptan benzoate (RBZ) loaded solid lipid nanoparticles (SLNs) for improved *ex-vivo* permeation. RBZ loaded SLNs were formulated by hot high pressure homogenization method. SLNs were characterized for size, zeta potential and scanning electron microscopy (SEM). The RBZ SLNs comprising mucoadhesive buccal film were fabricated using dependent variables in different concentration of Eudragit RS100 and HPMC K4M by using solvent evaporation method. The formulations were experimentally optimized using two factors, three level statistical design approach. The formulated buccal film comprising RBZ SLNs evaluated for mucoadhesive strength, swelling index, drug release and *ex vivo* permeation. The optimized formulation of RBZ SLNs showed particle size, polydispersity index, zeta potential and entrapment efficiency i.e. 228 nm, 0.22±0.02, -14mV, 81.78% respectively. Optimized mucoadhesive buccal film formulation followed Korsmeyer-Peppas drug release kinetic model with non-Fickian diffusion mechanism. Flux, lag time, permeability values in *ex vivo* permeation of RBZ from SLNs loaded film were found to be 0.071µg/cm<sup>2</sup>.h, 60 min., 0.014 respectively. The flux and permeability values were increased and lag time for permeation was decreased in *ex vivo* permeation studies of RBZ SLNs buccal film as compared to RBZ film. The results of the *in vitro* and *ex vivo* permeation study advocate the mucoadhesive film comprising RBZ SLNs is encouraging approach for drug delivery to brain targeting diseases.

**Keywords:** Solid Lipid nanoparticles; Rizatriptan benzoate; Buccal film; Bioavailability.

**Article Info:** Received 04 May 2019; Review Completed 06 June 2019; Accepted 10 June 2019; Available online 15 June 2019



### Cite this article as:

Salve P, Bali N, Fabrication and optimization of buccal film comprising rizatriptan benzoate loaded solid lipid nanoparticles for improved *ex vivo* permeation, Journal of Drug Delivery and Therapeutics. 2019; 9(3-s):636-648  
<http://dx.doi.org/10.22270/jddt.v9i3-s.3112>

### \*Address for Correspondence:

Dr. Pramod S. Salve, Department of Pharmaceutical Sciences, Rashtrasant Tukadoji Maharaj Nagpur University, Nagpur (M.S.) India-440033

### INTRODUCTION

Nanoparticles (NPs) are objects in the size range 1-1000 nm [1]. NPs favours for transport across biomembranes due to their physical properties. The favourable property linked to NPs includes multifunctionalization and higher payloads. The rationale for development of NPs for brain disorders includes their ability to cross blood-brain barrier (BBB). The phenomenon depends on physicochemical properties of NPs rather than chemical structure of the embedded drug. The more acceptability of NPs is due to their chemical and biological stability. The higher loading of both hydrophilic and lipophilic drugs makes them more feasible for development of oral, inhalational, and parenteral dosage forms [2].

The stable lipid-based nanocarriers provide a hydrophobic core for the drug to be dissolved or dispersed in it [3]. The solid lipid nanoparticles (SLNs) are comprised of triglycerides, fatty acids, and waxes. The size range varies

between 40-200 nm which favours to cross the tight endothelial cells of BBB and avoid the reticuloendothelial system (RES) [4]. The molten lipid-containing drug is dispersed in an aqueous solution by high-pressure homogenization (HPH) leading to generation of microemulsion. The advantages of SLNs are their biocompatibility, higher drug entrapment efficiency and provide continuous drug release for weeks [5].

Migraine is an episodic syndrome results from dysfunctioning of sympathetic nervous system [6]. The etiology of migraine is not well understood. The suggested mechanisms of migraine are neurovascular theory and cortical spreading depolarization theory [7]. The symptoms of migraine are one sided primary headache, vomiting, nausea and environmental reactivity [8].

Oral drug delivery being highly patient compliant also suffers from the hepatic first pass metabolism [9,10]. The oral route has some disadvantage for certain drugs due to extensive

pre-systemic metabolism in liver, which often leads to lack of significant correlation between membrane permeability, absorption and bioavailability [11].

Buccal route provides the direct access to systemic circulation through the jugular vein bypassing the hepatic first-pass metabolism leading to enhanced bioavailability of drug. Other advantages of buccal route includes excellent accessibility, low enzymatic activity, painless administration, easy withdrawal, addition of permeation enhancer/enzyme inhibitor or pH modifier in buccal formulations, versatility in designing as multidirectional or unidirectional release systems for local or systemic action [12]. Recently, the nanoparticles based buccal drug delivery system has generated increased interest. The advantages of solid lipid nanoparticles in combination with advantage of buccal route of drug administration can result in enhanced permeation across buccal mucosa [13].

The buccal films provide the advantage of small size thinness, flexibility resulting in patient compliance as compared to tablets. The buccal films can maintain extensive contact with buccal mucosa to enhance the bioavailability of drug [14].

RBZ is an anti-migraine and anti-inflammatory agent used in the treatment of acute migraine attacks. It stimulates presynaptic 5-HT<sub>1D</sub> receptors, which serves to inhibit both vasodilatation and inflammation. After oral administration, it undergoes extensive hepatic first-pass metabolism to inactive indole acetic acid derivative resulting into decreased bioavailability (~45%) [15].

The available researches on solid lipid nanoparticles containing RBZ have been reported by [16]. The mucosal drug delivery of RBZ has been reported by [17]. The buccal drug deliveries of RBZ using solid lipid nanoparticles have not been investigated or characterized and clear need exists for development of RBZ embedded SLNs. In order to enhance the buccal permeation of RBZ, we envisaged to develop and characterize the buccal film containing RBZ embedded SLNs.

## MATERIALS AND METHOD

### Materials

RBZ was obtained as a gratis sample from Mylan Laboratories, Hyderabad, India. Stearic acid and tween 80 were obtained from Merck India Ltd, India. Eudragit RS100 was obtained as gift sample from Evonik Industries, India. HPMC K4M was kindly received from Colorcon, India. All other chemicals and solvents were of analytical grade and

were procured from Merck India Ltd. All the materials were used as received. Purified water was obtained using Milli-Q water purification system.

### Methods

#### Differential scanning calorimetry (DSC) studies

DSC thermogram of RBZ, stearic acid and their physical mixture were recorded using Mettler-Toledo DSC apparatus, Zurich, Switzerland. A sample (5 mg) was weighed into aluminium pans and subjected to heating at a rate of 10 °C/min from 30 °C to 400 °C. Nitrogen gas at a flow rate of 40 ml/min was used as a purge gas in DSC analysis [18].

#### FT-IR spectrometry studies

In FT-IR studies, RBZ and stearic acid were individually triturated and mixed well with potassium bromide in 1:1 ratio. The samples were compressed under 10 t/nm<sup>2</sup> pressure and scanned in 400 to 4000 cm<sup>-1</sup> stretching frequency range. The FT-IR spectrum of physical mixture was compared with spectrum of RBZ and stearic acid. The shift in the stretching frequency of RBZ in presence of stearic acid was investigated to determine physical interactions between RBZ and stearic acid [19].

#### Solubility studies of drug in lipids

Stearic acid, 1g was added to test tube and heated in a controlled temperature water bath at 80 °C. RBZ was added in to molten stearic acid with gentle shaking till molten phase was saturated with it. Solubility of drug was determined in mg/g of lipid. Same procedure was followed for glyceryl monostearate, compritol 888 ATO. The lipid which showed maximum solubility of RBZ was selected for preparation of SLNs [20].

#### Preparation of drug loaded SLNs

SLNs were prepared by high pressure homogenization method with some modifications [21,22]. Stearic acid was melted and kept in water bath at 80 °C. In the molten lipid phase, weighed amount of RBZ was added. The aqueous phase was comprised of tween 80 dissolved in purified water, previously heated at 80 °C. The molten hot lipid phase was dispersed in hot surfactant phase and obtained the pre-emulsion under high speed homogenizer (Ultra turrax T18, IKA, Germany) at 14000 rpm at 80 °C for 4 min. The warm pre-emulsion was introduced in high pressure homogenizer at 500 bar pressure for 6 cycles to form the SLNs dispersion. The SLNs dispersion formed was allowed to cool at room temperature (Table 1).

**Table 1** Formulation Composition

Sr. No	Ingredients	AR1	AR2	AR3
1	Rizatriptan benzoate (mg)	80	80	80
2	Stearic acid (%w/w)	3	3	3
3	Tween 80 (%v/v)	1	2	3
4	Distilled water	q.s	q.s	q.s

### Freeze-drying of SLNs

The SLNs dispersion was mixed with 3 %w/v mannitol as cryoprotectant and subjected to deep freezing at (-) 60 °C. The frozen sample was moved for drying process in freeze-dryer. The drying period was conducted for 72 h by applying 100 mTorr vacuum. The freeze dried SLNs were used for analysis and incorporation in buccal films.

### Characterization of lyophilized SLNs

#### Particle size and zeta potential

For measurement of particle size of SLNs, a 5 mg sample of lyophilized SLNs was dispersed in 10 ml deionized water. The mean diameter, polydispersity index and zeta potential values were determined using Malvern Zetasizer Nano ZS, Malvern Instrument (Malvern, UK) [23,24].

### Entrapment efficiency and loading capacity

A back calculation method was used for measurement of entrapment efficiency. In an allomer tube, 2 ml dispersion was placed and centrifuged at 80,000 rpm for 45 min. at 4 °C. The amount of RBZ in aqueous medium was estimated spectrophotometrically at 232 nm. The percent entrapment efficiency (%EE) and percent drug loading (%DL) of RBZ were calculated as per equation (2) and (3) respectively [25].

$$\% EE = \frac{\text{Amount of RBZ added} - \text{amount of RBZ in supernatant}}{\text{Amount of RBZ added}} \times 100$$

Equation (2)

$$\% DL = \frac{\text{Amount of RBZ added} - \text{amount of RBZ in supernatant}}{\text{Amount of RBZ added} - \text{amount of RBZ in supernatant} + \text{Amount of lipid added}} \times 100$$

Equation (3)

### DSC studies

DSC thermogram of RBZ, stearic acid, RBZ-stearic acid physical mixture and RBZ embedded SLNs were recorded using a differential scanning calorimeter DSC 823 Mettler Toledo, Mettler Ltd. The thermal behaviour was studied by heating  $2.0 \pm 0.2$  mg of individual sample in a covered sample pan under nitrogen gas flow. The thermograms were recorded over the temperature range 30 °C - 300 °C at a heating rate of 10 °C/min. The thermogram of RBZ was compared with thermograms of physical mixture and SLNs [26].

### FT-IR spectrometry

The FT-IR spectra of RBZ, stearic acid and RBZ embedded SLNs were recorded using Shimadzu-IR AFFINITY FT-IR spectrophotometer. The samples were triturated and mixed well with potassium bromide in 1:1 ratio. The triturated sample was introduced in sample holder and scanned in the range 4500-500  $\text{cm}^{-1}$ . The spectrum of SLNs was compared to the spectra of RBZ, lipid and their physical mixtures [25].

### Scanning electron microscopy (SEM)

The surface morphology and structure were visualized by scanning electron microscopy (SEM) (EVO 18, Carl Zeiss, Germany). SEM images of RBZ and SLNs were recorded after coating with gold/palladium in vacuum beforehand at 2 and 20 KeV accelerating voltage [27].

### Preparation of SLNs loaded buccal film

Buccal films containing RBZ SLNs were prepared by solvent casting technique [28]. The calculated amount of HPMC K4M was dispersed 10 ml 95 %v/v ethanol with continuous stirring using magnetic stirrer in a separate beaker. To it, polyethylene glycol 400 was added as a plasticizer in proportion to 30 %w/w of polymer weight. The weighed amount of Eudragit RS100 was dissolved in 10 ml 95 %v/v ethanol and to it triethyl citrate was added as a plasticizer in proportion to 20 % w/w of polymer weight. The above two solutions were mixed. The calculated amount of RBZ SLNs was incorporated in the mixed polymeric solution after levitation. The bubbles were removed with aid of sonicator. The solution was casted onto petri dish and dried at 25 °C for 24 h. The glass transition temperature of Eudragit RS100 is in the range 28-32 °C, hence the film was dried well below its glass transition temperature. The films were cut into size of diameter 1.5 cm containing SLNs equivalent to 5 mg RBZ. The prepared films were packed in aluminium foil and stored in an airtight glass container to maintain the integrity and elasticity of films.

### Experimental design

A full factorial design for two factors at three levels each was selected to optimize response of variables. The two factors, the mucoadhesive polymer (g) and sustained release polymer (g) used were varied and the factor levels were suitably coded. The % cumulative release, mucoadhesive strength and swelling index were taken as the response variables. In the design, the two factors were evaluated each at three levels and experimental trials were performed for possible combinations. All other formulation variables and processing variables were kept constant throughout the studies.

The formulae were developed as 9 sets varying the variables following  $3^2$  full factorial design (3 levels) using Design expert. Dependent variables were Y1 = % cumulative release, Y2 = mucoadhesive strength and Y3= swelling index. The effect of two independent variables HPMC K4M (X1) and Eudragit RS100 (X2) on the responses (Y1, Y2, Y3) were observed. The levels of all other ingredients in the formulation were fixed.

### Evaluation of buccal films

#### Film thickness

The thickness of buccal film was measured at four corners and in centre of film (total five locations using dial gauge.) Average of five readings was taken as thickness of film [29].

#### Folding endurance

The folding endurance was measured manually for prepared films. Films were repeatedly folded at the same place till it breaks. The number of times the film could be folded at the same place without breaking was the folding endurance value [30].

#### Surface pH study

Buccal films were allowed to swell for 2 h in pH 6.8 phosphate buffer solution. The glass electrode of pH meter was placed on the surface of the swollen film. A mean of three pH readings was recorded [12].

#### Swelling index

Buccal film was kept in a petri dish containing 50 ml of pH 6.8 phosphate buffer solution. The cover slip was removed and weighed after each hour till period of 6 h. The difference in the weights was recorded as weight gain due to absorption of water. The swelling index of film as per equation (4)

$$\% S = \frac{W_2 - W_1}{W_1} \times 100 \quad \dots\dots\dots(4)$$

Where,  $W_2$  is the weight or area of the swollen film after time t and  $W_1$  is the original film weight [31].

#### Determination of drug content

The films were investigated for RBZ content uniformity by UV spectrophotometry [31]. Circular pieces of films of 1.5 cm diameter were cut from three different places from the casted film. Each sample film piece was placed in 100 ml volumetric flask and dissolved in pH 6.8 phosphate buffer. From it, 0.2 ml was withdrawn and diluted with pH 6.8 phosphate buffer up to 10 ml. The absorbance of solution was measured at 225 nm using uv/visible spectrophotometer (Shimadzu UV-1700). The percent RBZ content was determined using standard calibration curve and procedure was repeated for three films of each formulation.



### *Ex Vivo mucoadhesive strength*

A modified balance method was used for determining the *ex vivo* mucoadhesive strength. Fresh goat buccal mucosa was obtained from a local slaughterhouse and used within two hours of slaughter. The mucosal membrane was separated by removing the underlying fat and loose tissues. The membrane was washed with distilled water and then with pH 6.8 phosphate buffer. A piece of buccal mucosa was pasted to the glass beaker using an instant adhesive and held on the right side of the balance. The film was stuck to the lower side of the glass petri dish with instant adhesive. The right hand pan was balanced by adding weights on the left hand pan. Weights were slowly added to the left-hand pan until the film was detached from the mucosal surface. The weight in gram required to detach the film from the mucosal surface was recorded as the mucoadhesive strength [32].

### *Ex Vivo permeation study*

The *ex vivo* buccal permeation studies of RBZ film and RBZ embedded SLNs film were performed using a Franz diffusion cell at  $37 \pm 0.5$  °C. A fresh goat buccal mucosa was obtained from local slaughter house and used within two hours of slaughter. Freshly obtained goat buccal mucosa of 1.77 cm<sup>2</sup> surface area was mounted between the donor and receptor compartments. The buccal film containing RBZ and RBZ SLNs were individually placed on the mucosal side and the compartments were clamped together. The receptor compartment (20 ml capacity) was filled with pH 6.8 phosphate buffer and the hydrodynamics in the compartment was maintained by stirring at 50 rpm with a magnetic bead. A 3 ml sample was withdrawn at predetermined time intervals and analyzed for RBZ content by uv/visible spectrophotometer using blank [28].

### *Dissolution study*

The dissolution studies of SLNs embedded buccal films were carried using USP Dissolution Test Apparatus Type -II. The films were attached mid-way of test apparatus using adhesive glue. The dissolution medium used was 500 ml of simulated saliva fluid maintained at  $37 \pm 0.5$  °C and stirred at 50 rpm. The samples were withdrawn after every 30 minutes and replaced with an equal volume of fresh dissolution media. The withdrawn samples were analyzed spectrophotometrically at 225 nm [33].

## RESULTS AND DISCUSSION

### *Differential scanning calorimetry (DSC)*

The DSC thermogram of RBZ shown an endothermic with onset at 179.63 °C and end set at 182.79 °C. The endothermic melting was observed at 180.84 °C. The corresponding enthalpy value was found to be (-) 122.69 Jg<sup>-1</sup> (Fig 1 A). Stearic acid shown melting endotherm at 57.70 °C with onset at 55.63 °C and end set at 60.83 °C. The corresponding enthalpy for thermal transition was found to be (-) 252.02 Jg<sup>-1</sup> (Fig 1B). The endotherm of physical mixture of RBZ and stearic acid in 1:1 ratio shown the melting endotherm at 57.70 °C with onset at 55.63 °C and end set at 60.03 °C. The corresponding enthalpy value was found to be (-) 251.02 Jg<sup>-1</sup> (Fig 1C). The lyophilized SLNs containing RBZ shown an endothermic endotherm at 65.94 °C with onset at 90.96 °C and end set at 112.82 °C with enthalpy value of (-) 255.20 Jg<sup>-1</sup> (Fig 1D).

The shifting of melting endotherm of RBZ from 180.84 °C to 57.70 °C was observed in DSC studies of physical mixture of RBZ with stearic acid. It indicated the complete solubilization of drug in the stearic acid. Similarly, the enthalpy value of RBZ was found to be decreased from (-) 122.6 to (-) 251.02

Jg<sup>-1</sup> which was near to enthalpy of stearic acid i.e. (-) 252.02 Jg<sup>-1</sup>. In case of the lyophilized SLNs containing RBZ, the melting endotherm was shifted to lower temperature at 65.94 °C. The enthalpy value in case of lyophilized SLNs containing RBZ was found to be near to the enthalpy of stearic acid and physical mixture. The above observations concluded the complete solubilization of RBZ in stearic acid phase has occurred.

### *FT-IR studies*

In the FT-IR studies, the characteristic stretching frequencies of RBZ viz. N-H stretching at 2920 cm<sup>-1</sup>, C=N stretching at 1640 cm<sup>-1</sup> were observed (Fig 2A). The stretching frequencies of stearic acid viz. O-H stretching (carboxylic acid) at 2848cm<sup>-1</sup>, O-H stretching (alcohol) at 3600 cm<sup>-1</sup> were observed (Fig 2B). The characteristic stretching frequencies of RBZ were found to be disappeared due to interaction with stearic acid (Fig 2C). The disappearance of stretching frequencies of RBZ indicated its solubilization in stearic acid.

### *Solubility studies of drug in lipids*

Solubility of drug in lipid determines the degree of drug loading in lipid. The lipids were screened for solubility of RBZ at 70 °C. The solubility of drug in glyceryl monostearate, stearic acid, compritol 888 ATO was found to be  $48.9 \pm 0.67$ ,  $92. \pm 0.96$ ,  $11.8 \pm 0.88$  mg/g of solid lipid respectively. As solubility of drug was maximum in stearic acid, it was used for preparation of SLNs.

### *Preparation of SLNs*

This study reports a hot high pressure homogenization process for preparation of RBZ SLNs and investigates effect of surfactant concentration on drug loading.

### *Characterization of SLNs*

SLNs provide prolong stability, drug release control and incorporates hydrophilic and lipophilic drugs. The prepared SLNs were subjected to particle size and zeta potential measurements.

### *Particle size*

The formulations AR1, AR2, and AR3 showed the decrease in particle size with an increase in surfactant concentration [34]. The increasing concentration of surface active agent decreases surface tension and provides stability to created particles during homogenization process [35]. The formulation batches AR<sub>1</sub>, AR<sub>2</sub> and AR<sub>3</sub> contained tween 80 in 1, 2 and 3 %w/v concentration respectively. The particle size of formulations AR<sub>1</sub>, AR<sub>2</sub> and AR<sub>3</sub> were found to be 509.6 nm, 253.9 nm, and 228.9 nm respectively. The surfactant tween 80 in 3 %w/v concentrations showed decreased particle size (AR<sub>3</sub>) as compared to formulations AR<sub>1</sub> and AR<sub>2</sub> containing 1 and 2 % w/v tween 80. Similarly, the polydispersity index (PDI) of formulations was found to decrease with an increase in tween 80 concentrations. The optimized formulation AR<sub>3</sub> shown PDI value 0.493 which was the least value as compared to formulations AR<sub>1</sub> and AR<sub>2</sub>. Formulation AR<sub>3</sub> was subjected to lyophilization process. The particle size distribution graph of formulation AR<sub>3</sub> is shown in figure 3A.

### *Zeta potential*

The zeta potential is measure of surface charge present on the particles. The zeta potential values of formulations studied was found to range from (-) 1.4 to (-) 14 mV indicating that the agglomeration of particle was not occur. The formulations AR<sub>1</sub>, AR<sub>2</sub> and AR<sub>3</sub> showed an increase in zeta potential value with an increase in tween 80 concentrations [36]. Colloidal dispersions with zeta potential

values in the range (-) 30 mV to (+) 30 mV are considered to be stable (Fig 3B). The formulation AR3 was selected as optimized formulation having (-) 14 mV zeta potential value.

#### *DSC studies of lyophilized SLNs*

In DSC studies, a melting endotherm of RBZ was observed at 180.34 °C. The melting endotherm of stearic acid was observed at 57.24 °C. The comparison of melting endotherm clearly concludes the shifting of endotherm to lower temperature, 65.94 °C. It indicates formation of SLNs. The enthalpy value in case of lyophilized SLNs containing RBZ was found to be near to the enthalpy of stearic acid and physical mixture. The above observations concluded the complete solubilization of RBZ in stearic acid phase has occurred.

#### *FT-IR spectrometry studies of lyophilized SLNs*

In the FT-IR spectrum of lyophilized SLNs, an intermolecular interaction between SLNs and mannitol was observed as indicated by O-H stretching at 2848 cm<sup>-1</sup>. This stretching frequency was observed due to the formation of a hydrogen bond between the O-H group of the mannitol with polar head group of stearic acid (Fig 2D).

#### *SEM studies of lyophilized SLNs*

Scanning electron microscopic (SEM) image of RBZ and SLNs are shown in figure 4A and 4B respectively. In the SEM image of RBZ, irregular shape particles in 20 µm magnification were observed. Whereas, SEM image of lyophilized SLNs shown a perfectly spherical solid lipid nanoparticles in 100 nm magnification. The SLNs were found to be smooth and surface integrity was observed.

#### **Preparation of SLNs loaded buccal film**

Previous reported studies revealed buccal films containing RBZ. We developed buccal films containing RBZ embedded SLNs using a blend of HPMC K4M and Eudragit RS100 polymers. The films were found to be smooth, thin, and flexible. The surface of the films was found to be fairly homogeneous with limited entrapped air bubbles. The films containing drug embedded SLNs were found to be slightly opaque as compared to films containing SLNs.

#### **Experimental design**

The formulations were prepared as 9 sets using two variables following 3<sup>2</sup> factorial designs. Buccal films containing SLNs were prepared by solvent evaporation technique.

The optimized formulations selected by the design were prepared and the parameters were compared to the expected values. The results are shown in table 3. For systematic investigation of the factors, a full factorial design was employed.

The effect on % cumulative release (Y1) was observed to be significant by ANOVA and the polynomial equation was found to follow equation 5.

$$Y_1 = 81.14 - 3.53333A - 10.6233B + 1.3325AB \text{ -----(5)}$$

The terms A and B indicate concentrations of polymers HPMC K4M and Eudragit RS100 respectively. As shown in equation 5, the negative sign with terms A and B indicated an inverse relationship between concentration of polymers and % CR. As the concentrations of both polymers were increased, the % CR was found to be decreased. For response Y1 as shown in table 4, the coefficient of determination value (R<sup>2</sup>) was found to be 0.9068 indicating a good fit agreement between concentrations of polymers and % CR. The surface

response (3D) plot of % CR and its contour plot are shown in figure 5A and 5B respectively.

The effect on mucoadhesive strength (Y2) was observed to be significant by ANOVA and the polynomial equation was found to follow equation 6.

$$Y_2 = 28.8178 + 6.42A - 3.57B + 1.54AB \text{ -----(6)}$$

The term A indicates concentration of HPMC K4M whereas, term B indicates concentration of Eudragit RS100. By analyzing the equation, the positive response was observed for mucoadhesive strength with HPMC K4M. In case of Eudragit RS100, a negative response indicating the decreased mucoadhesive strength was observed with an increase in Eudragit RS100 concentration. The coefficient of determination was found to be value (R<sup>2</sup>) 0.9924 indicated the best fit agreement between effect of polymers on mucoadhesive strength. The surface response (3D) plot of mucoadhesive strength and its contour plot are shown in figures 5C and 5D respectively.

The effect on swelling index (Y3) was observed to be significant by ANOVA and the polynomial equation was found to follow equation 7.

$$Y_3 = 77.7511 + 12.9633A - 10.9183B + 4.4325AB \text{ -----(7)}$$

The term A indicates concentration of HPMC K4M whereas term B indicates concentration of Eudragit RS100. By analyzing the equation, a positive response was observed for swelling index with increasing concentration of HPMC K4M. In case of Eudragit RS100, a negative response indicating the decreased swelling index was observed with an increase in Eudragit RS100. The coefficient of determination (R<sup>2</sup>) was found to be 0.9235 indicating the good fit agreement between effects of polymers on swelling index. The surface response (3D) plot of swelling index and its contour plot are shown in figures 5E and 5F respectively.

The p-values for % cumulative release, mucoadhesive strength and swelling index were found to be 0.005, < 0.0001 and 0.0032 respectively. Thus the P-values were found to be significant. The results of statistical analysis are shown in table 4.

#### **Evaluation of buccal film containing RBZ loaded SLNs**

##### *Film thickness and folding endurance*

The thickness of buccal film (PF8) were found to be 0.29 ± 0.99 mm. Folding endurance was considered adequate to reveal good film properties. The films showed folding endurance values in the range 199-228 [37].

##### *Surface pH and swelling index*

The surface pH of buccal film was found to be 6.7 ± 0.003. The importance of swelling property lies in the bioadhesion phenomenon. The bioadhesion of film on mucous membrane occurs due to swelling, disentanglement and relaxation of polymer chains [38,31]. The hydration rate and water uptake in the formulation F4 was found to be highest. The maximum proportion of HPMC K4M and minimum proportion of Eudragit RS100 favoured more water penetration resulting in enhanced swelling. The swelling index of formulations F4 was found to be 95.77 ± 2.89% (Fig. 8)

##### *Mucoadhesive strength*

Adhesive force determines mucoadhesive property. The mucoadhesion theory involves diffusion and water penetration in polymeric film. The faster rates of hydration and swelling equilibrium of films are important factors for mucoadhesive property [39,40]. The increased swelling index of film was found to contribute to enhanced

mucoadhesion. The nanoparticle size in SLNs contributed for faster water penetration and resulted in mucoadhesive force. The water solubility of RBZ played significant role by permitting more water influx in films. As the amount of HPMC K4M was increased, the mucoadhesion was found to be increased. The increasing amount of Eudragit RS100 has shown decreasing mucoadhesive strength due to its hydrophobic character. Peak detachment force is the maximum applied force at which the film detaches from membrane. The mucoadhesive strength for formulation F4 was found to be  $37.63 \pm 1.99$  g. In this formulation the HPMC K4M in its highest proportion contributed to the swelling and penetration of the film in the mucous membrane resulting in enhanced mucoadhesion (Fig 9).

#### Ex vivo diffusion study

In the ex vivo diffusion studies of film containing RBZ and RBZ loaded SLNs, the flux, lag time and permeability values were determined. The lag time for permeation of RBZ film was found to be 90 min. The RBZ embedded SLNs film has shown lag time of 60 minutes. The drug diffusion was found to increase from film formulations containing RBZ embedded SLNs. The film containing SLNs shown enhanced drug diffusion across skin as compared to be film containing RBZ. The inclusion of RBZ embedded SLNs was found to enhance diffusion across skin as compared to the diffusion of RBZ. The drug diffusion was found to vary from 44 to 97 % in 300 min diffusion studies (table 5). The flux value for film containing RBZ was found to be  $0.045 \text{ mg/cm}^2\text{h}$ . The SLNs embedded RBZ film formulation shown the flux value  $0.071$

$\text{mg/cm}^2\text{h}$ . The permeability values were obtained by dividing the flux values of RBZ films and SLNs embedded RBZ films by the donor phase concentration of the drug present in film i.e. 5 mg RBZ. The permeability values found to be 0.009 and 0.0142 for RBZ film and SLNs embedded RBZ films respectively. The difference factor in the permeability was found to be 0.0052. An enhancement by 57.8 % in the permeability value was observed in SLNs embedded formulation as compared to RBZ formulation (Fig 7).

#### In vitro drug release studies

The in vitro release studies were carried up to 300 min. The amount of drug release was found to vary from 65.63 to 95.14 % (table 3). In the first hour of release studies, less than 20 % drug release was observed in formulations containing 150 mg Eudragit RS100 (formulations F5, F6, and F8). The formulations containing 50 mg Eudragit RS100 has shown faster dissolution profile as evidenced in formulations F3, F4, F9. An increasing proportion of Eudragit RS 100 was found to retard the drug release. The formulation F8 shown a better control on drug release from film formulation and hence considered as optimized formulation (Fig 6). Formulation F8 contained HPMC K4M as a hydrophilic sustained release polymer and Eudragit RS100 as hydrophobic release retarding agent. The effect of the hydrophobic and hydrophilic characteristic of polymers used in film contributed for the drug release control. The optimized formulation F8 showed Korsmeyer-Peppas drug release kinetic model with non-Fickian diffusion mechanism as a best fit model. The  $R^2$  value was found to be 0.9910.

**Table 2** Percent Encapsulation Efficiency and loading Capacity of Formulations (AR1 - AR3)

Formulation code	% RBZ loading	% Encapsulation efficiency
AR1	$4.99 \pm 0.45$	$70.10 \pm 0.56$
AR2	$5.85 \pm 0.42$	$76.11 \pm 0.33$
AR3	$6.55 \pm 0.32$	$81.78 \pm 0.32$

**Table 3** Experimental Design and Parameters for  $3^2$  Factorial Design

Formulation Batches	HPMC K4M (mg)	Eudragit RS100 (mg)	Cumulative Release (%)	Swelling Index (%)	Mucoadhesive Strength (g)
F1	300	100	$86.46 \pm 1.77$	$67.81 \pm 3.09$	$23.39 \pm 2.17$
F2	500	100	$81.27 \pm 2.39$	$92.38 \pm 2.64$	$34.73 \pm 3.06$
F3	400	50	$90.36 \pm 1.73$	$92.11 \pm 1.37$	$32.56 \pm 2.91$
F4	500	50	$84.47 \pm 2.93$	$95.77 \pm 2.89$	$37.63 \pm 1.99$
F5	300	150	$72.97 \pm 3.53$	$53.12 \pm 2.24$	$16.82 \pm 2.67$
F6	400	150	$65.63 \pm 2.85$	$58.69 \pm 1.64$	$25.58 \pm 2.86$
F7	400	100	$86.33 \pm 3.11$	$73.26 \pm 2.60$	$28.04 \pm 2.42$
F8	500	150	$67.63 \pm 2.98$	$88.59 \pm 3.19$	$33.49 \pm 1.88$
F9	300	50	$95.14 \pm 3.77$	$78.03 \pm 2.30$	$27.12 \pm 3.13$

Values expressed as mean  $\pm$  S.D., n = 3.

**Table 4** ANNOVA for response surface quadratic model for optimization of mucoadhesive buccal film

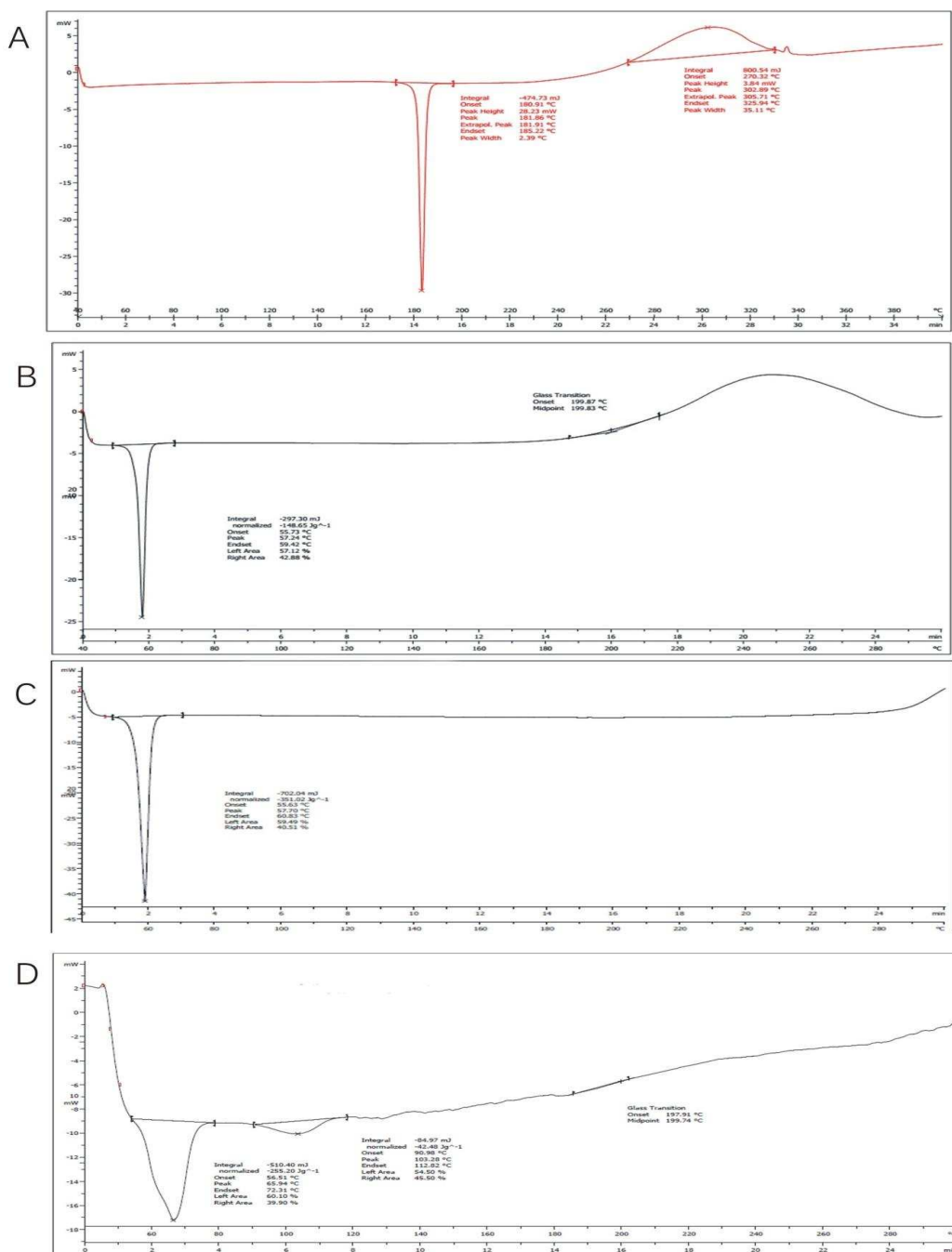
Response	Model	DF	CI	SE	P-Value	SD	R <sup>2</sup> Value
Y1	2FI	1	87.61	1.87	0.005	3.95	0.9068
Y2	2FI	1	32.92	0.34	<0.0001	0.72	0.9924
Y3	2Fi	1	88.47	2.58	0.0032	5.46	0.9235

Y1= Cumulative Release, Y2= Mucoadhesive Strength, Y3= Swelling Index, CI= Class Interval, SE= Standard Error, P= Calculated Probability, SD= Standard Deviation, R<sup>2</sup>= Coefficient of Determination

**Table 5** Percent Diffused of RBZ and RBZ SLNs from Film

Time (min)	% Cumulative RBZ diffused from film	% Cumulative RBZ diffused from film containing SLNs
0	0.0000	0.000
30	1.4850 ± 3.57	1.900 ± 2.98
60	1.8700 ± 4.11	2.530 ± 3.86
90	2.3000 ± 3.58	13.693 ± 2.74
120	5.6900 ± 2.38	21.663 ± 2.64
150	11.5700 ± 3.06	30.561 ± 2.37
180	17.0530 ± 3.55	37.512 ± 3.92
210	24.2300 ± 4.39	46.592 ± 3.22
240	32.3000 ± 3.44	51.450 ± 2.97
270	37.1490 ± 3.95	59.506 ± 4.27
300	42.0100 ± 2.70	66.015 ± 3.51

Values expressed as mean ± S.D., n = 3.

**Fig. 1** Represents DSC thermogram of RBZ (A), stearic acid (B), physical mixture of RBZ and stearic acid (C) and lyophilized SLNs comprising RBZ (D). Thermal behavior of lyophilized SLNs showed that complete solubilization of RBZ in stearic acid



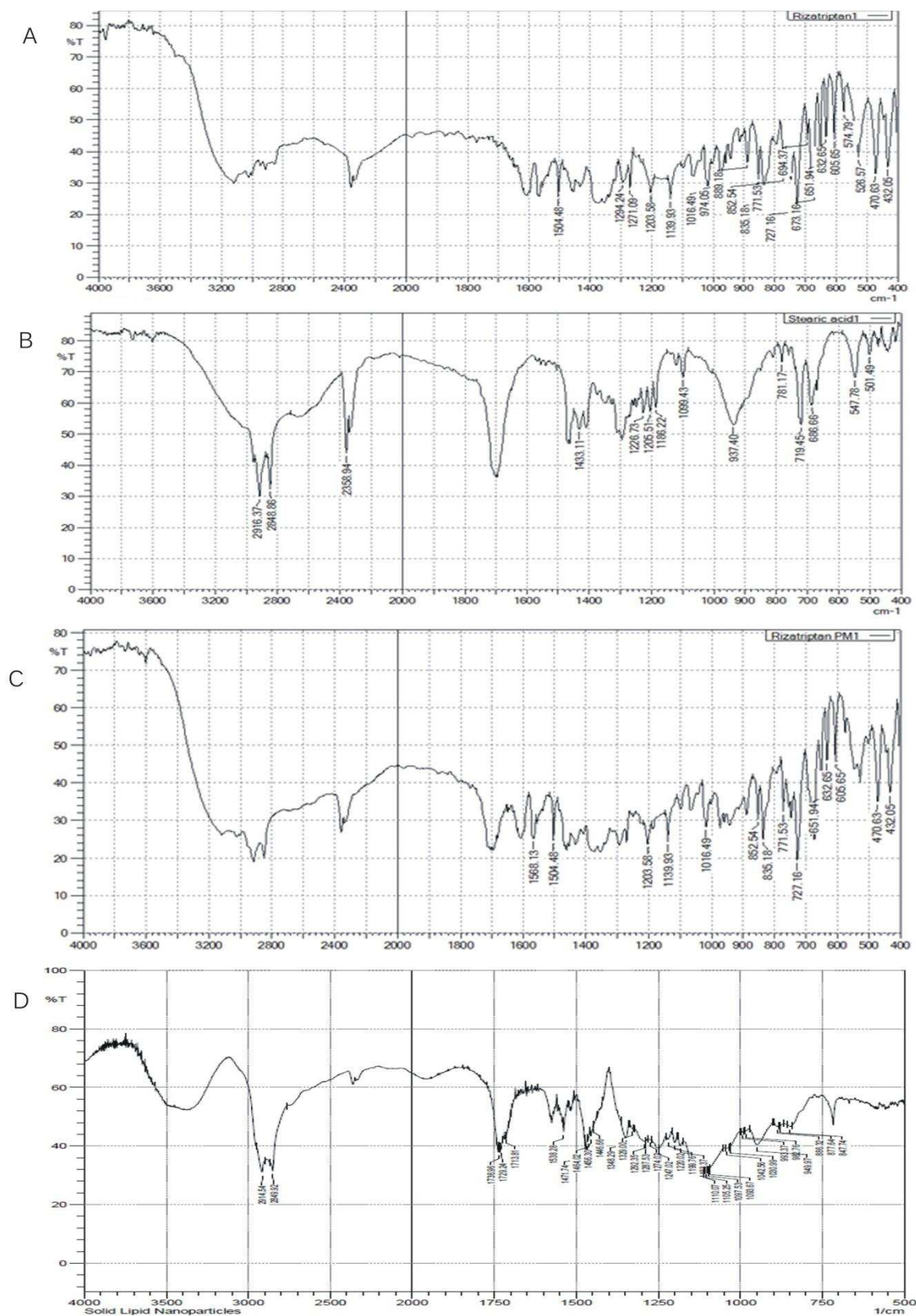


**Fig. 2** FTIR spectra for RBZ (A), stearic acid (B), physical mixture of RBZ and stearic acid (C) and lyophilized SLNs comprising RBZ (D) showing characteristic peaks at various numbers



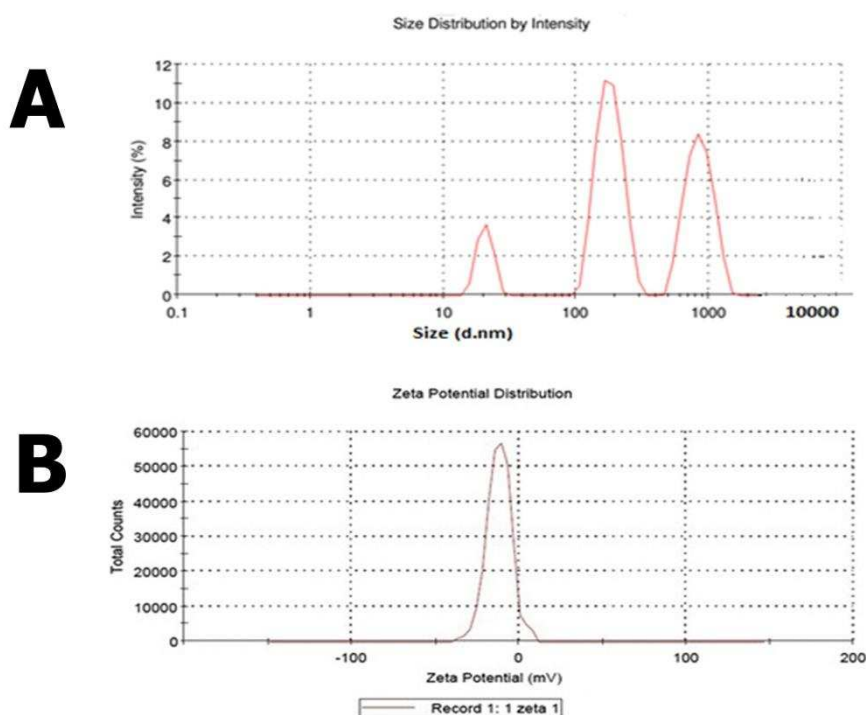


**Fig. 3** Intensity-based particle size distribution for RBZ comprising SLNs (A) with dynamic light scattering on zetasizer® and zeta potential distribution for RBZ comprising SLNs (B) with respect to total counts measured using zetasizer® software

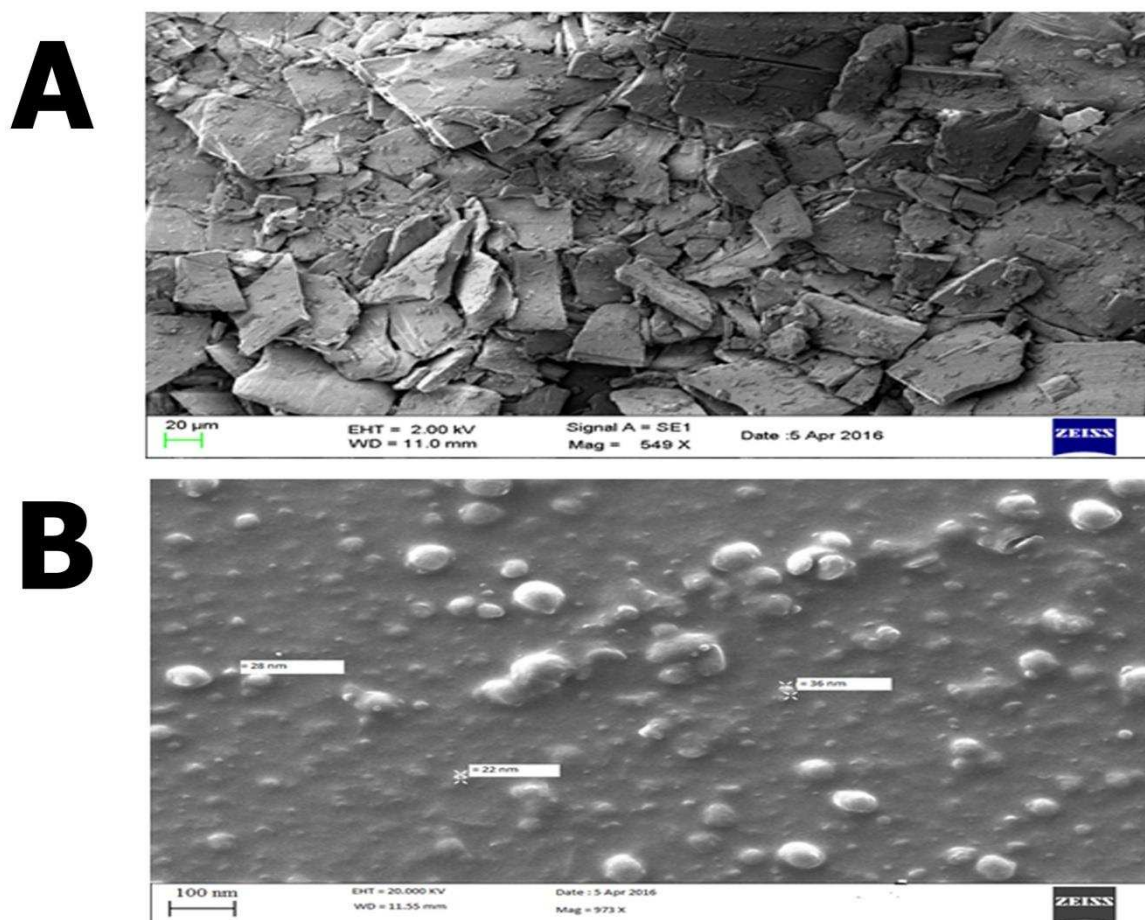


**Fig. 4** Scanning electron microscopic images of RBZ showing bulk irregular shape phases (A), and lyophilized RBZ SLNs (B) showed spherical shape particles. Scale bar: A-20 µm, B-100 nm

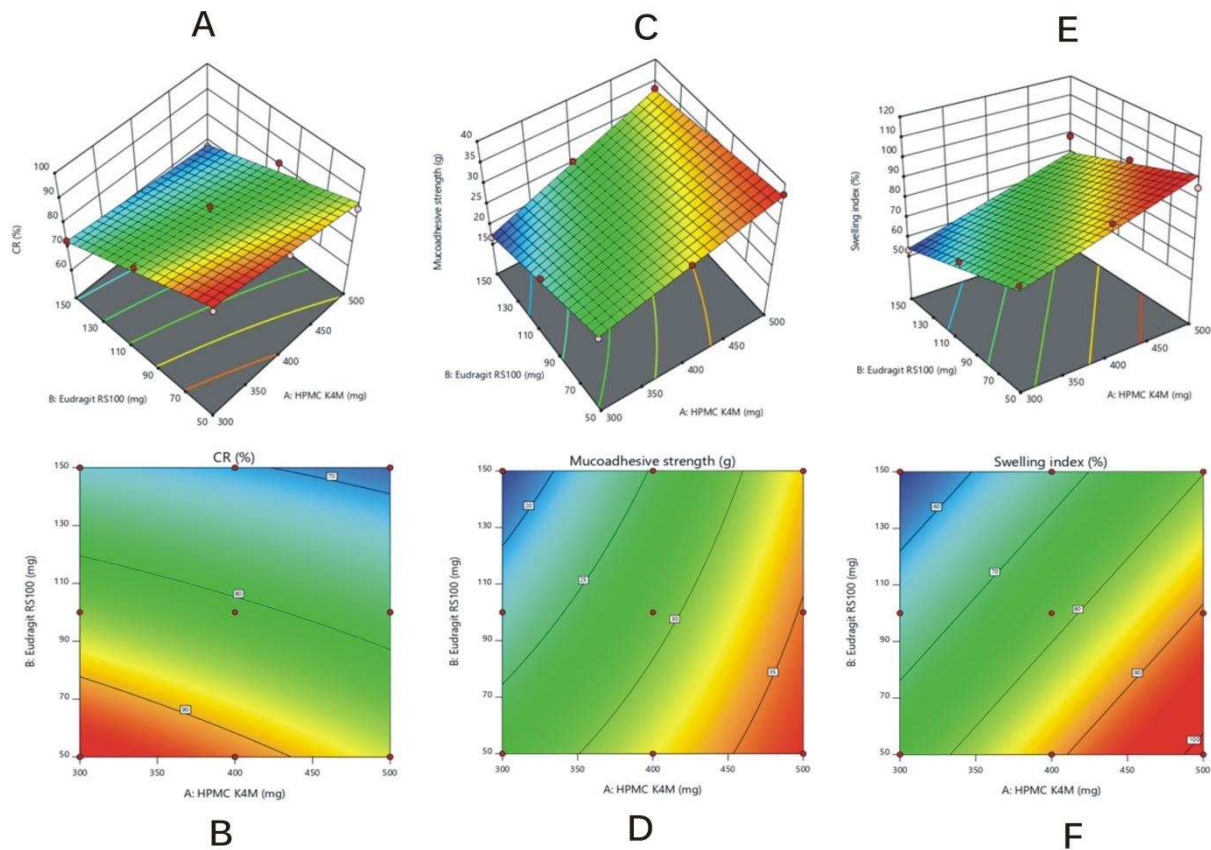


**Fig. 5** The response surface plot (A,C,E) and contour plot (B,D,F) showing relationship between concentration of HPMC K4M ( $X_1$ ) and Eudragit RS100 ( $X_2$ ) on cumulative release ( $Y_1$ ), mucoadhesive strength ( $Y_2$ ) and swelling index ( $Y_3$ ). (A,B): effect of ( $X_1$ ) and ( $X_2$ ) on ( $Y_1$ ); (C,D): effect of ( $X_1$ ) and ( $X_2$ ) on ( $Y_2$ ); (E,F): effect of ( $X_1$ ) and ( $X_2$ ) on ( $Y_3$ ).

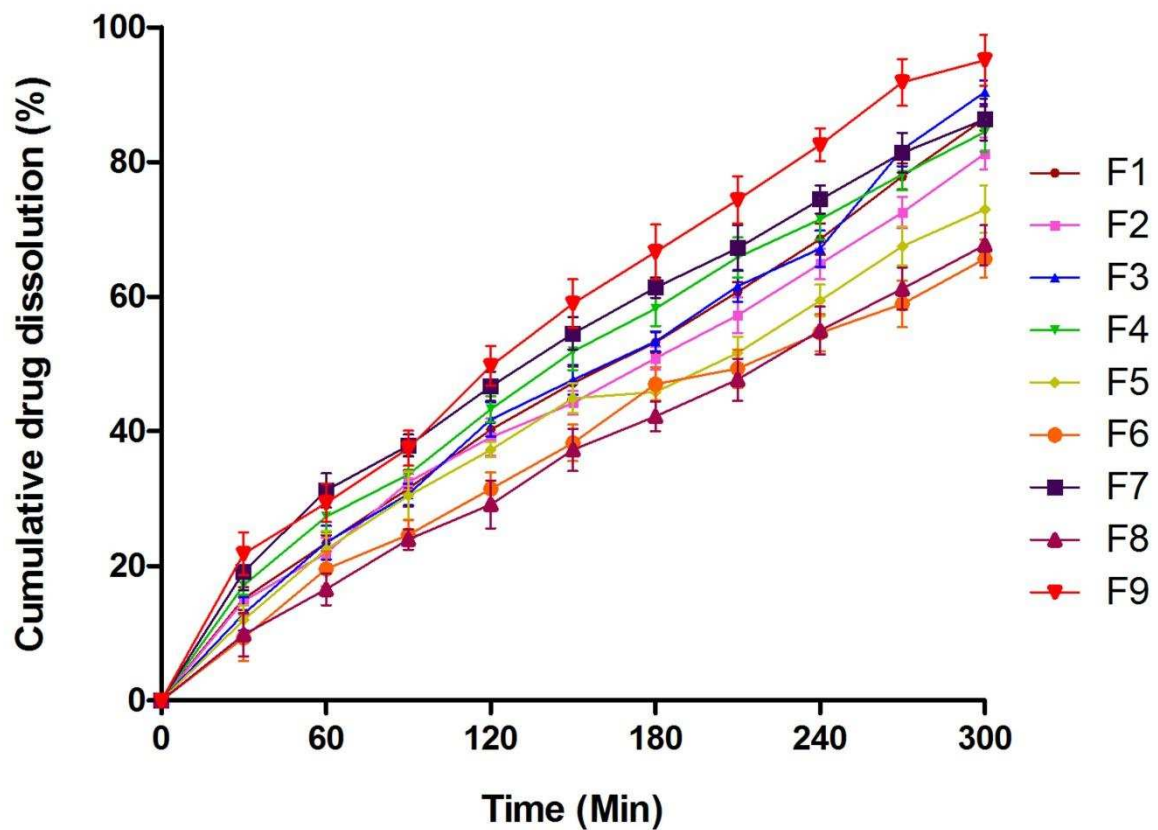


**Fig. 6** Represents the cumulative drug dissolution. Effect of different concentration of Eudragit RS100 i.e. 50 mg, 100 mg, 150 mg on formulation batches F1 to F9. *In vitro* drug dissolution pattern was studied by USP dissolution test apparatus

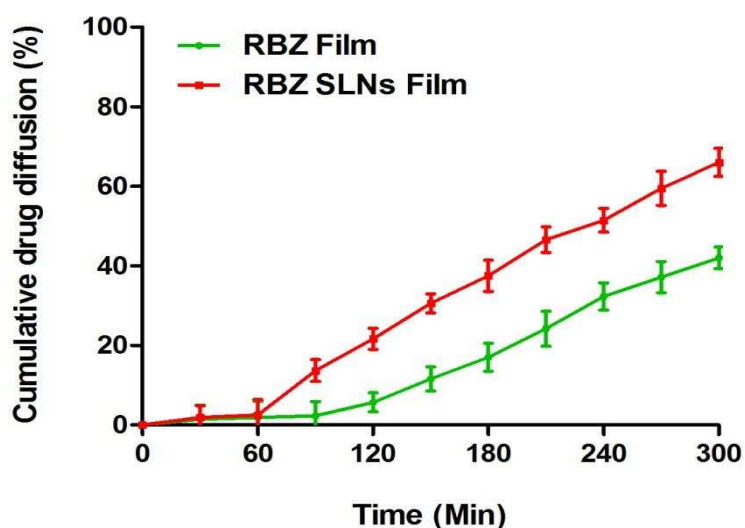


**Fig. 7** Represents the cumulative drug diffusion. Effect of RBZ film and RBZ SLNs comprising film showed the lag time and significance difference on permeability. Drug diffusion pattern was studied by Franz diffusion cell at  $37 \pm 0.5^\circ \text{C}$

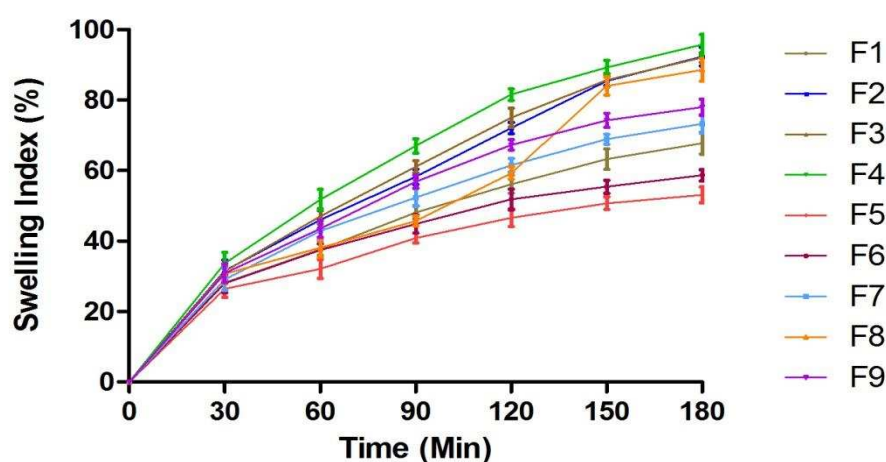


**Fig. 8** Represents the swelling index. Effect of different concentrations of HPMC K4M i.e. 300 mg, 400 mg, 500 mg on formulation batches F1 to F9. Swelling index pattern was studied at different time interval

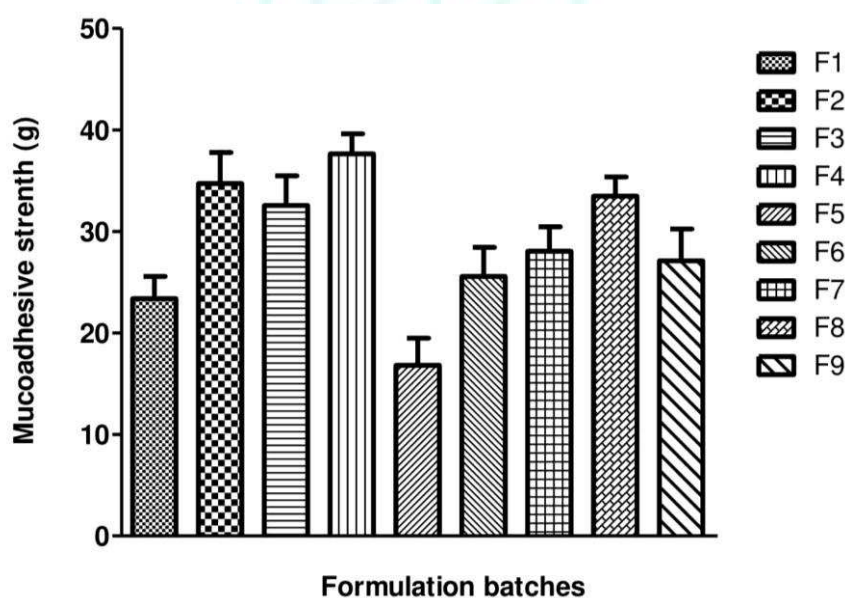


**Fig. 9** Represents the mucoadhesive strength. Effect of different concentration of HPMC K4M i.e. 300 mg, 400 mg, 500 mg on formulation batches F1 to F9. Mucoadhesive strength pattern was studied by modified balance method



## CONCLUSION

The aim of this study was to develop buccal film formulations containing RBZ embedded SLNs. The objectives were to identify the optimal parameters like lipid solubility, surfactant concentration, particle size, zeta potential, mucoadhesive strength, and ex vivo diffusion. Also the objective was to compare the ex vivo diffusion of RBZ embedded SLNs with the buccal film containing RBZ. In this study, the ex vivo permeation of RBZ embedded SLNs were conducted. The highest solubility of RBZ was found in stearic acid. In preformulation work, the DSC and FT-IR studies revealed complete solubilization of RBZ in stearic acid. SLNs were prepared using tween 80 as a surfactant in varying concentration. A reduction in particle size was observed with tween 80. A least particle size distribution averaging to 228.9 nm was observed with 3 %w/v tween 80. The zeta potential value of (-) 14 mV was observed with 3 % tween 80 providing stability to the SLNs. The zeta potential value of developed SLNs was found to increase with an increase in tween 80 concentration. The SEM image of lyophilized SLNs shown regular spherical size solid lipid nanoparticles with smooth surface. The optimized batch of SLNs was used for optimization of formulation of buccal patch using 3<sup>2</sup> full factorial designs. Mucoadhesive strength was found to be increased with increased HPMC K4M concentration. The maximum mucoadhesion was observed with minimum concentration of Eudragit RS100 used in preparation of buccal films. Similarly the swelling index was found to increase with an increase in HPMC K4M. Mucoadhesion and swelling index studies were found to increase the permeation of RBZ across buccal mucosa. The response plots for percent cumulative release, mucoadhesive strength and swelling index were found to follow 2FI of statistical analysis model. The ex vivo permeation of RBZ embedded SLNs buccal film was found to be enhanced as compared to RBZ buccal film. The release kinetic study revealed that optimized formulation followed Korsmeyer-Peppas drug release kinetic model with non-Fickian mechanism. The developed RBZ loaded SLNs formulation makes it more convenient to cross the blood brain barrier. Hence provides the promising approach for the delivery of RBZ in the brain.

## Conflict of interest

The authors declare that they have no conflict of interest.

## Acknowledgement

The authors gratefully acknowledge the Mylan laboratories, Hyderabad, India for providing Rizatriptan benzoate. Also authors are thankful to Evonik Industries and Colorcon, India for proving Eudragit RS100, HPMC K4M respectively.

## REFERENCES

- [1] Youns, M., Hoheise, J.D., Efferth, T.: Therapeutic and diagnostic applications of nanoparticles. *Curr. Drug. Targets.* 12(3), 357-65 (2011)
- [2] Petkar, K.C., Chavhan, S.S., Agatonovik-Kustrin, S., Sawant, K.: Nanostructured materials in drug and gene delivery are view of the state of the art. *Crit. Rev. Ther. Drug. Carrier. Syst.* 28(2), 101-64 (2011)
- [3] Kaur, I.P., Bhandari, R., Bhandari, S., Kakkar, V.: Potential of solid lipid nanoparticles in brain targeting. *J. Control. Release.* 127(2), 97-109 (2008)
- [4] Pardeshi, C., Rajput, P., Belgamwar, V., Tekade, A., Patil, G., Chaudhary, K., Sonje, A.: Solid lipid based nanocarriers: An overview. *Acta. Pharm.* 62(4), 433-7 (2012)
- [5] Mishra, B., Patel, B.B., Tiwari, S.: Colloidal nanocarriers: a review on formulation technology, types and applications toward targeted drug delivery. *Nanomedicine: Nanotechnology, Biology and Medicine.* 6(1): 9-24 (2010)
- [6] Peroutka, S.J. Migraine: A chronic sympathetic nervous system disorder. *Headache the Journal of Head and Face Pain.* 44(1), 53-64 (2004)
- [7] Hauge, A.W., Asghar, M.S., Schytz, H.W., Christensen, K., Olesen, J.: Effects of tonabersat on migraine with aura: a randomised, double-blind, placebo-controlled crossover study. *Lancet. Neurol.* 8(8),718-723 (2009)
- [8] Kristoffersen, E.S., Lundqvist, C.: Medication-overuse headache: epidemiology, diagnosis and treatment. *Ther. Adv. Drug. Saf.* 5(2), 87-99 (2014)
- [9] Hamman, J.H., Enslin, G.M., Kotze, A.F.: Oral delivery of peptide drugs: barriers and developments. *BioDrugs.* 19(3), 165-177 (2005)
- [10] Shaji, J., Patole, V.: Protein and peptide drug delivery: oral approaches. *Indian. J. Pharm. Sci.* 70(3), 269-277 (2008)
- [11] Harris, D., Robinson, J.R.: Drug delivery via the mucous membranes of the oral cavity. *J. Pharm. Sci.* 81(1), 1-10 (1992)
- [12] Shidhaye, S.S., Saindane, N.S., Sutar, S., Kadam, V.: Mucoadhesive bilayered patches for administration of sumatriptan succinate. *AAPS. PharmSciTech.* 9(3), 909-916 (2008)
- [13] Rana, P., Murthy, R.S.: Formulation and evaluation of mucoadhesive buccal films impregnated with carvedilol nanosuspension: a potential approach for delivery of drugs having high first-pass metabolism. *Drug. Deliv.* 20(5), 224-235 (2013)
- [14] Abruzzo, A., Federica, B., Teresa, C., Federica, C., Beatrice, V., Barbara, L.: Mucoadhesive chitosan/gelatin films for buccal delivery of propranolol hydrochloride. *Carbohydrate Polymers.* 87(1), 581-588 (2012)
- [15] Keny, R.V., Desouza, C., Lourenco, C.F.: Formulation and evaluation of rizatriptan benzoate mouth disintegration tablet. *Indian. J. Pharm. Sci.* 72(1), 79-85 (2010)
- [16] Girotra, P., Singh, S.K.: Multivariate optimization of rizatriptan benzoate-loaded solid lipid nanoparticles for brain targeting and migraine management. *AAPS PharmSciTech.* 18(2), 517-528 (2017)
- [17] Salehi, S., Boddohi, S.: New formulation and approach for mucoadhesive buccal film of rizatriptan benzoate. *Prog. Biomater.* 6(4): 175-187 (2017)
- [18] Rarokar, N.R., Saoji, S.D., Khedekar, P.B.: Investigation of effectiveness of some extensively used polymers on thermoreversible properties of Pluronic® tri-block copolymers. *J. Drug. Dev. Sci. Tech.* 44, 220-230 (2018)
- [19] Rarokar, N.R., Saoji, S.D., Raut N.A., Taksande, J.B., Khedekar, P.B., Dave, V.S.: Nanostructured cubosomes in a thermoresponsive depot system: an alternative approach for the controlled delivery of docetaxel. *AAPS. Pharm. SciTech.* 17(2), 436-445 (2015)
- [20] Mendes, A.I, Silva, A.C., Catita, J.M., Cerqueira, F., Gabriel, C., Lope, C.M.: Miconazole-loaded nanostructured lipid carriers (NLC) for local delivery to the oral mucosa: Improving antifungal activity. *Colloids. Surf. B. Biointerfaces.*111,755-763 (2013)
- [21] Blasi, P., Schoubben, A., Traina, G., Manfroni, G., Barberini, L., Alberti, P.F., Cirotto, C., Ricci, M.: Lipid nanoparticles for brain targeting III. Long-term stability and *in-vivo* toxicity. *Int. J. Phar.* 454(1), 316-323 (2013)
- [22] Shegokar, R., Singh, K.K., Müller, R.H.: Production & stability of stavudine solid lipid nanoparticles-from lab to industrial scale. *Int. J. Pharm.* 416(2), 461-470 (2011)
- [23] Wissing, S.A., Muller, R.H., Manthei, L., Mayer, C.: Structural characterization of Q10-loaded solid lipid nanoparticles. *Pharm. Res.* 21(3), 400-405 (2004)



- [24] Asasutjarit, R., Lorenzen, S.I., Sirivichayakul, S., Ruxrungtham, K., Ruktanonchai, U., Ritthidej, G.C.: Effect of solid lipid nanoparticles formulation compositions on their size, zeta potential and potential for *In Vitro* pHIS-HIV-Hugag transfection. *Pharm. Res.* 24(6), 1098-1107 (2007)
- [25] Barman, R.K., Iwao, Y., Funakoshi, Y., Ranneh, A.H., Noguchi, S., Wahed, M.I., Itai, S.: Development of highly stable nifedipine solid-lipid nanoparticles. *Chem. Pharm. Bull.* 62(5), 399-406 (2014)
- [26] Bhalekar, M., Upadhaya, P., Madgulkar, A.: Formulation and characterization of solid lipid nanoparticles for an anti-retroviral drug darunavir. *Applied. Nanoscience.* 7(1-2), 47-57 (2017)
- [27] Sharma, G., Jasuja, N.D., Kumar, M., Ali, M.I.: Biological synthesis of silver nanoparticles by cell-free extract of *spirulina plantesis*. *J. Nanotech.* 1-6 (2015)
- [28] Adhikari, S.N.R., Nayak, B.S., Nayak, A.K., Mohanty, B.: Formulation and evaluation of buccal films for delivery of atenolol. *AAPS. PharmSciTech.* 11(3), 1038-1044 (2010)
- [29] Verma, N., Wahi, A.K., Verma, A., Chattopadhyay, P.: Evaluation of a mucoadhesive buccal patch for delivery of atenolol: *in vitro* screening of bioadhesion. *J. Pure. Appl. Microbiol.* 1(1), 115-18 (2007)
- [30] Nafee, N.A., Boraie, M.A., Ismail, F.A., Mortada, L.M.: Design and characterization of mucoadhesive buccal patches containing cetylpyridinium chloride (CPC). *Acta. Pharma.* 53(3), 199-212 (2003)
- [31] Semalty, A., Semalty, M., Nautiyal, U.: Formulation and evaluation of mucoadhesive buccal films of enalapril maleate. *Indian. J. Pharm. Sci.* 72(5), 571-575 (2010)
- [32] Patel, V.M., Prajapati, B.G., Patel, M.M.: Design and characterization of chitosan-containing mucoadhesive buccal films of propranolol hydrochloride. *Acta Pharm.* 57(1), 61-72 (2007)
- [33] Perioli, L., Ambrogi, V., Angelici, F., Ricci, M., Giovagnoli, S., Capuccella, M., Rossi, C.: Development of mucoadhesive patches for buccal administration of ibuprofen. *J. Control. Release.* 99(1), 73-82 (2004)
- [34] Dalvi, S.V., Dave, R.N.: Controlling particle size of a poorly water-soluble drug using ultrasound and stabilizers in antisolvent precipitation. *Ind. Eng. Chem. Res.* 48(16), 7581-7593 (2009)
- [35] Ostertag, F., Weiss, J., McClements, D.J.: Low-energy formation of edible nanoemulsions: factors influencing droplet size produced by emulsion phase inversion. *J. Colloid. Interface. Sci.* 388(1), 95-102 (2012)
- [36] Upadhyay, S., Pate, J., Patel, V., Saluja, A.: Effect of different lipids and surfactants on formulation of solid lipid nanoparticles incorporating tamoxifen citrate. *J. Pharm. Bioallied. Sci.* 4(Suppl 1), S112-S113 (2012)
- [37] Kraisit, P., Limmatvapirat, S., Nunthanid, J., Sriyamornsak, P., Luangtana-Anan M.: Preparation and characterization of hydroxypropyl methylcellulose/polycarbophil mucoadhesive blend films using a mixture design approach. *Chem. Pharm. Bull.* 65(3), 284-294 (2017)
- [38] Garg, S., Kumar, G.: Development and evaluation of a buccal bioadhesive system for smoking cessation therapy. *Pharmazie.* 62(4), 266-272 (2007)
- [39] Kundu, J., Patra, C., Kundu, S.C.: Design, fabrication and characterization of silk fibroin HPMC-PEG blended films as vehicle for transmucosal delivery. *Mater. Sci. Eng. C.* 28(8), 1376-1380 (2008)
- [40] Giovino, C., Ayensu, I., Tetteh, J.: An integrated buccal delivery system combining chitosan films impregnated with peptide loaded PEG-b-PLA nanoparticles. *Colloids. Surf. B. Biointerfaces.* 112, 9-15 (2013)